

Early Warning of Heat/Cold Waves as a Smart City Subsystem: A Retrospective Case Study of Non-anticipative Analog Methodology

Dmytro Zubov

Tecnológico de Monterrey, School of Engineering and Sciences, San Luis Potosi Campus, Mexico
dzubov@ieee.org

Abstract

In this paper, a forecasting of the heat/cold waves is discussed as a subsystem of the smart city concept using the non-anticipative analog method. The prediction algorithm is described by two paradigms. First one (short range) uses quantum computing formalism. D-Wave adiabatic quantum computing Ising model is employed and evaluated for the forecasting of positive extremes of daily mean air temperature. Forecast models are designed with two to five qubits, which represent 2-, 3-, 4-, and 5-day historical data, respectively. Ising model's real-valued weights and dimensionless coefficients are calculated using daily mean air temperatures from 119 places around the world as well as sea level (Aburatsu, Japan). The proposed forecast quantum computing algorithm is simulated based on traditional computer architecture and combinatorial optimization of Ising model parameters for the Ronald Reagan Washington National Airport dataset with 1-day lead-time on learning sample 1975-2010 yr. Analysis of the forecast accuracy (ratio of successful predictions to total number of predictions) on the validation sample 2011-2014 yr shows that Ising model with three qubits has 100% accuracy, which is significant as compared to other methods. However, number of identified heat waves is small (only one out of nineteen in this case). Second paradigm (long range) uses classical computation in the Microsoft Azure public cloud. Here, the forecast method identifies the dependencies between the current values of two meteorological variables and the future state of another variable. The method is applied to the prediction of heat/cold waves at Ronald Reagan Washington National Airport. The data include standard meteorological variables from 119 places around the world, as well as sea level (Aburatsu, Japan), average monthly Darwin and Tahiti sea level pressures, SOI, equatorial SOI, sea surface temperature, and multivariate ENSO index (131 datasets in total). Every dataset is split into two samples, for learning and validation, respectively. Initially, the sum of the values at two different locations (minus corresponding expectation values) is calculated with lead-time from 14 to 365 days on summation interval of length from 1 to 365 days. Objective function defines the distribution based on two input datasets with appropriate lead-time and summation interval, which have maximum (or minimum) sum compared with the rest of data four times at least (with a minimum time difference of at least 30 days), when a later extreme event occurs in the learning sample. Specific extreme events at Ronald Reagan Washington National Airport were thus predicted on the validation sample, based on rules referring to events in earlier years. Some extremes are specifically predicted (up to 26.3% of all extremes). The methodology has 100% forecast accuracy with respect to the sign of predicted and actual values. Nowadays, the smart city project is developed at School of Engineering and Sciences (San Luis Potosi), Tecnológico de Monterrey. The early warning of heat/cold waves as well as technical aspect (remote control with Arduino Ethernet Shield and virtual power plant with solar energy are emphasized) are the main focuses of the Internet of Things project.

1. Introduction

We are living a time of Internet of Things' (IoT) intensive growth when ubiquitous computing connects different objects (e.g. cars, computers, fridges, lighting, industrial electronic machines) among each other and to people (Dirk Slama et al., 2015; Charalampos Doukas, 2012). IoT smart city (Luis Hernández et al., 2012; Hafeedh Chourabi et al., 2012) is the main approach to enhance quality and performance of urban services, to reduce costs and resource consumption, and to increase the usage of renewable resources. Lightweight hardware (e.g. Arduino Ethernet Shield; <https://www.arduino.cc/en/Main/ArduinoEthernetShield>) and software (e.g. MQTT IoT protocol; Valerie Lampkin et al. 2012) create a basis of smart city concept.

Success factor of smart city depends considerably on the structure and elements of its framework. The eight basic components include the following (Hafedh Chourabi et al., 2012): (1) management and organization, (2) technology, (3) governance, (4) policy, (5) people and communities, (6) the economy, (7) built infrastructure, and (8) the natural environment. Core to the concept of a smart city is the use of the weather forecasting in the natural environment component to increase sustainability and to better manage natural resources (Hafedh Chourabi et al., 2012; Smart Weather Solutions, 2013). The weather forecasting can be classified into five main groups based on lead-time: now casting (a period of 0 to 2 hours ahead), a very short range (up to 12 hours), a short range (12 to 72 hours), a medium range (72 to 240 hours), an extended range (beyond 10 days and up to 30 days description of weather parameters, usually averaged and expressed as a departure from climate values for that period), and a long range for the period from 30 days up to two years (<http://www.wmo.int/pages/prog/www/DPS/GDPS-Supplement5-AppI-4.html>).

Nowadays, the numerical forecast models show high accuracy for lead-times up to two weeks. However, the power grids (e.g. to reserve a gas for the peak of the energy consuming), the agriculture (e.g. to predict the best period for the planting), the medicine (e.g. to do the appropriate preventives for the period of heat wave when the number of cardiologic problems is increased dramatically), and some other branches need accurate predictions for the longer period (more than two weeks usually).

Nowadays, a large set of meteorological variables (air temperature, precipitation, wind, pressure, visibility, snow depth, etc.) is used for the forecasting at different locations (Kattsov, 2010). They interact constantly, and some variables may be evaluated using the others in accordance with known teleconnection patterns (Nada Pavlovic Berdon, 2013). Thus, the reasoning of forecast models must involve the full set of meteorological variables. However, temperature and precipitation are the targets of long-range forecasting mainly because of practical needs. Precipitation has a close relationship to air temperature and vice versa (Van Den Dool & Nap, 1985). Correlation analysis shows that precipitation forecasting is effective within two weeks, but air temperature over a much longer period (greater than a year; Zubov & Vlasov, 2004). The impact is increased further because extremes can be used for the correction of forecasted averages.

A wide spectrum of forecast models has now been developed (Vilfand, Tishenko, & Khan, 2003). They are usually classified into synoptic (Vorobiov, 1991), numerical (Belov, Borisenkov, & Panin, 1989), and statistical (Onwubolu et al., 2007) groups. The first two are used mainly for short- and medium-range forecasting mainly because they produce significant errors at long range and use highly complex equations. Heterogeneous algorithms are applied for the weather forecasting – seasonal time series (Qiang Song, 2011), neural networks (Gyanesh Shrivastava, 2012), probability theory (Sadokov, Kozelcova, & Kuznecova, 2011), ensemble forecasting (Astahova & Alferov, 2008), distinct scenarios of anthropogenic forcing (Bardin, 2011), dependency on ENSO cycle (Higgins, Kim, & Unger, 2004), self-organizing systems based on inductive modelling (Madala & Ivakhnenko, 2004), D-Wave adiabatic quantum computing Ising models (Amin, Neil G. Dickson, & Peter Smith, 2013), etc. The nonlinearity and sensitivity of existing forecast models, possible small errors in initial conditions (dust, sand, pollution, etc.), random observation errors, background states, and lack of data combine to reduce the forecast accuracy and complicate the design of models (Douglas & Phillip J. Englehart, 2007; Fathalla A. Rihan & Chris G. Collier, 2010; Tyndall et al., 2010).

Inductive self-organizing models show good results when enough of the right data is fundamentally not obtainable. In Zubov, 2013 was shown that robust highly accurate long-range forecasting of average daily air temperatures might be achieved using inductive modeling. The principle used in that work to predict high-impact weather events substantiates the interaction of different climate system components centered in different places. The first stage of the forecast reasoning model is the selection of three most data-related places using the Pearson product-moment correlation coefficient, which has to be greater than 0.8 in absolute value. The second stage

is finding weights of the forecast model to use with the inductive modeling objective function “minimum of regularity plus maximum of conjunctions” with a combinatorial algorithm. This approach corresponds to the teleconnections (Glantz, Katz, & Nicholls, 1991; Nada Pavlovic Berdon, 2013) because of a linkage between weather changes occurring in widely separated regions of the globe.

Public cloud Software-as-a-Service is a high-performance tool for NP-complex algorithms (Collier & Shahan, 2015). In particular, Windows Azure virtual machines (VMs) may host the NP-complex apps. If forecast software is developed using Windows Forms, VMs can use standard operating systems Windows Server 2008/2012 R2 to start executable files. However, reasoning of forecast models takes a lot of time – two weeks for one location approx. Hence, new concept using the adiabatic quantum computing is proposed for the computational process speed-up (Dahl, 2015; Smelyanskiy et al., 2012; McGeoch & Wang, 2013). Nowadays, different quantum computer types are discussed (e.g. quantum logic gates, one-way quantum computer, quantum cellular automata, topological quantum computer, adiabatic quantum computer), but only adiabatic quantum computer was built by D-Wave Systems Company. D-Wave One has its roots in a 16-qubit processor built in 2006. It led to the firm’s 28-qubit processor in 2007, and then its 128-qubit processor in 2010. D-Wave Two with 512-qubit processor was completed in 2013 (Dahl, 2015).

Hence, the main goal of this paper is to investigate the heat/cold waves’ early warning subsystem of smart city framework. A long-range forecasting non-anticipative analog methodology is the basic approach as well as cloud/quantum computation and lightweight IoT protocols. This project is a subpart of the intelligent algorithms’ development for the smart city at School of Engineering and Sciences, campus San Luis Potosi, Tecnológico de Monterrey. The work focuses the remote control with Arduino Ethernet Shield and virtual power plant with solar energy.

This paper is organized as follows: In Section 2, the principle of non-anticipative analog long-range forecasting of heat/cold waves based on the self-organizing approach is shown; Microsoft Azure cloud classical computation of the forecast models is discussed as well. In Section 3, D-Wave adiabatic quantum computing using Ising model is presented for the short-range forecasting of heat waves. In Section 4, the experiment with IoT MQTT lightweight protocol is described using heterogeneous hard- (Arduino Ethernet Shield and HP ProBook 650 G1 laptop) and software (Mosquitto MQTT broker, C# console and Arduino apps). Conclusions are summarized in Section 5.

2. Principle of the non-anticipative analog long-range forecasting of heat/cold waves using Microsoft Azure cloud high-performance computing

It is assumed that some event (or group of events) $A(j)$ has an impact on another event $B(j')$, where $B(j')$ – extreme air temperature (defined as two standard deviations away from the climatologic baseline), j, j' – event dates and $(j' - j) > 0$. The correlation analysis (Zubov, 2013) shows that enough of the right data for the average daily air temperatures is not obtainable in principle. In this case, four-fold repetitions of extreme air temperatures for a give lead time $(j' - j)$ after the same $A(j)$ on the learning sample is taken to establish the validity of $A(j)$ as a predictor. The dependency thus discovered is used as objective function for prediction. A non-anticipative long-range forecast methodology will be illustrated by the Ronald Reagan Washington National Airport air temperature extremes.

NOAA Satellite and Information Service (<http://www7.ncdc.noaa.gov/CDO/cdo>) is used as a main free data source from 1973 to 2014, providing 119 average daily air temperature datasets from around the world, Ronald Reagan Washington National Airport’s mean visibility in miles, mean wind speed in knots, mean dew point in Fahrenheit, maximum and minimum temperatures in Fahrenheit reported during the day, Darwin and Tahiti sea level pressures, southern oscillation index (SOI), equatorial SOI, sea surface temperature, multivariate ENSO index (average monthly). In addition, sea level data (Aburatsu, Japan; <http://ilikai.soest.hawaii.edu/woce/wocesta.html>; average daily) is used. Hence, 131 datasets are taken into consideration – $X_i = \{x_{i1}, x_{i2}, \dots, x_{ij}, \dots\}$, $i = \overline{1, 131}$, $j = \overline{1, 15340}$ ($j=1$ corresponds to Jan 1, 1973, $j=15340$ – to Dec 31, 2014; some stations are presented

in Table 1). These datasets and resources were selected because of free public access, air temperature daily averages, and data archives since 1973 at least. Nowadays, the statistic of extreme temperature anomalies is incomplete, which does not allow to use the detailed weather data generators (Adelard et al., 2000). Preprocessing standardizes the data using climatological values (baseline) \bar{x}_{ij} calculated as expectations for the appropriate date from Jan 1, 1973 to Dec 31, 2013 (e.g. $x_{114,4}=39.3^0\text{F}$, $\bar{x}_{114,4}=37.5^0\text{F}$, $x_{114,4}^*=-1.8^0\text{F}$):

$$x_{ij}^* = x_{ij} - \bar{x}_{ij}. \quad (1)$$

A value is considered extreme if the difference between this value and its expectation is greater than two standard deviations (SD) in absolute units. Considering the Ronald Reagan Washington National Airport dataset, positive x_{114,j_+}^+ ($j_+ = \overline{1,364}$) and negative x_{114,j_-}^- ($j_- = \overline{1,309}$) air temperature extremes are studied on the learning sample ($x_{114,j_+}^+, x_{114,j_-}^- \in E, E - \text{set of extremes}$). Data are split into learning (from 1975 to 2010: $j = \overline{731,13879}$; years 1973 and 1974 are reserved because of lead-time l and summation interval of length n which are up to one year each) and validation (from 2011 to 2014: $j = \overline{13880,15340}$) samples.

Table 1. Some stations (i.e. number of datasets) around the world, which are used for the forecast models' design.

i	Country or region	Station (named by NOAA)	i	Country or region	Station (named by NOAA)
1	Algeria	Annaba	113	United Kingdom	Heathrow Airport
2	American Samoa	Tafuna-Pago International AP	114	USA	Ronald Reagan Washington National Airport
3	Antigua And Barbuda	V C Bird INTL	115	Uruguay	Carrasco INTL
4	Argentina	MinistroPistarini INTL	116	Uzbekistan	Yuzhniy
5	Aruba	Reina Beatrix INTL	117	Vanuatu	Aneityum
6	Australia	Canberra Airport	118	Venezuela	Simon Bolivar INTL
...	119	Vietnam	Danang INTL

Considering the Ronald Reagan Washington National Airport dataset, the objective function that defines an event $A(j)$ as a precursor to an extreme event $B(j')$ is based on situations on the learning sample where

$$\sum_{k=0}^{n-1} (x_{i_1,(j'-k-l)}^* + x_{i_2,(j'-k-l)}^*) \Big|_{\substack{i_1, i_2 \in I \\ x_{114,j'} \in E \\ j' = [731,13879] \\ l \in L \\ n \in N}} > \text{Max} \vee \sum_{k=0}^{n-1} (x_{i_1,(j'-k-l)}^* + x_{i_2,(j'-k-l)}^*) \Big|_{\substack{i_1, i_2 \in I \\ x_{114,j'} \in E \\ j' = [731,13879] \\ l \in L \\ n \in N}} < \text{Min}, \quad (2)$$

$$\text{Max} \equiv \max_{\substack{i_1, i_2 \in I \\ j = [731,13879] \\ x_{114,j} \notin E}} \sum_{k=0}^{n-1} (x_{i_1,(j-k-l)}^* + x_{i_2,(j-k-l)}^*) \Big|_{\substack{i_1 = [1,131] \\ i_2 = [1,131] \\ l = [14,365] \\ n = [1,365]}}, \text{Min} \equiv \min_{\substack{j = [731,13879] \\ x_{114,j} \notin E}} \sum_{k=0}^{n-1} (x_{i_1,(j-k-l)}^* + x_{i_2,(j-k-l)}^*) \Big|_{\substack{i_1 = [1,131] \\ i_2 = [1,131] \\ l = [14,365] \\ n = [1,365]}}$$

(k – temporal summation index (days); n – length of summation interval (days); $l = j' - j$ – lead-time (days); $i_1, i_2 \in I$, $n \in N$, $l \in L$ for interrelated sets $I \subset [1,131]$, $N \subset [1,365]$, $L \subset [14,365]$ of meteorological variables, possible lengths of summation intervals, and lead-times, respectively). Cardinality of a set I equals two because of high computational complexity of the proposed non-anticipative analog algorithm. The sets I , N , and L encompass the precursor events $A(j)$ for a given

extreme event $B(j')$, for $j = j' - l$. A given event is defined by a unique tuple (i_1, i_2, n, l) together with Min and Max . Then, input datasets i_1 and i_2 with appropriate lead-time l and summation interval of length n are selected to define a prediction rule if the sum of meteorological variables from datasets i_1 and i_2 is greater than maximum Max (or less than minimum Min) four times at least (with a time difference greater than 30 days) on the learning sample, for cases where $x_{114,j'}^* \in E$ only, i.e. where there is an extreme event $B(j')$ at day j' . Hence, every extreme selection rule includes six parameters – the indices of two datasets i_1 and i_2 , the lead-time l , the summation interval of length n , maximum Max , and minimum Min . Max and Min are computed as the maximum and minimum values of the sums over the datasets i_1 and i_2 , with the same summation interval n and lead-time l , where an extreme event does not occur on the learning sample ($i=114$ is the index of the Ronald Reagan Washington National Airport dataset, and has to be altered for prediction of extreme events in other locations).

A non-anticipative analog method consists of four main steps:

1. Generation of the prediction rules.
2. Analysis of the prediction rules. The rules with time slots, which are not concentrated at the same frame, are excluded.
3. Generation of possible extremes.
4. Analysis of the generated possible extremes. The extremes with time slots, which do not correspond to the time slots of the appropriate rules, are excluded.

The results of the heat/cold waves' prediction from 2011 to 2014 at different locations (places are selected randomly) are presented in Table 2.

Table 2. Forecast accuracy of the heat/cold waves' predictions from 2011 to 2014 at different locations.

i	Country or region	Station (named by NOAA)	Forecast accuracy for the heat waves, %	Forecast accuracy for the cold waves, %
1	Algeria	Annaba	36.4	0
22	China	Beijing	0	28.6
70	Macedonia	Skopje	0	7.1
96	Russia	Dolgoprudnyj	0	7.7
112	Ukraine	Zhulyani	0	33.3
114	USA	Ronald Reagan Washington National Airport	26.3	0

Analysis of the presented in Table 2 results shows that heat waves can be predicted with accuracy up to 36.4%, cold waves – up to 33.3%. In addition, this methodology has 100% accuracy with respect to the sign of predicted and actual values (Zubov, 2015).

The forecast software was developed using Windows Forms and Delphi integrated development environment. Hence, VMs can use standard operating systems Windows Server 2008/2012 R2 to execute files. In Jul 2014, presented methodology got the Microsoft Research Climate Data Award, which allowed to design the Microsoft Azure public cloud with 32 processors Intel(R) Xeon(R) E5-2660 2.20 GHz. The six D-series VMs from Climate Data Award as well as one A-series standard tier VM from Windows Azure Educator grant (two Intel(R) Xeon(R) E5-2673 2.4 GHz) have been designing the forecast models. Azure management portal and screen shot of the VM are shown in Fig. 1.

Visualization of the forecasted data is based on Google Earth virtual globe (Kelly L. Murdock, 2009). Here, KMZ file represents the geographic placemarks in Google Earth. KMZ loads web-site faster because it is a compressed form of KML file. Prototype was developed using ASP.NET technology and hosted in Windows Azure public cloud against <http://gearth.azurewebsites.net>. Screenshot is shown in Fig. 2.

3. D-Wave quantum computing Ising model: a case study for the short-range forecasting of heat waves

Nowadays, only D-Wave Systems Company produces commercially the 2nd generation adiabatic quantum computer with up to 512 flux qubits (project code name "Vesuvius"). They are microscopic loops of niobium metal that are capable of quantum behavior at low temperatures. Hence, electrical currents in the loops can flow in clockwise (+1) or counterclockwise (-1) direction, or both, when in quantum superposition. Qubits are connected to neighbors according to the topology of quantum processor. The hardware is controlled by a framework of Josephson junctions that allow individual qubit values to be stored and read, and to influence the states of neighboring qubits. D-Wave computer uses quantum annealing to minimize the dimensionless energy of an Ising model

$$M(\mathbf{s}|\mathbf{h},\mathbf{J})= \sum_{m \in V(G)} h_m s_m + \sum_{(m,n) \in E(G)} J_{m,n} s_m s_n, \quad (3)$$

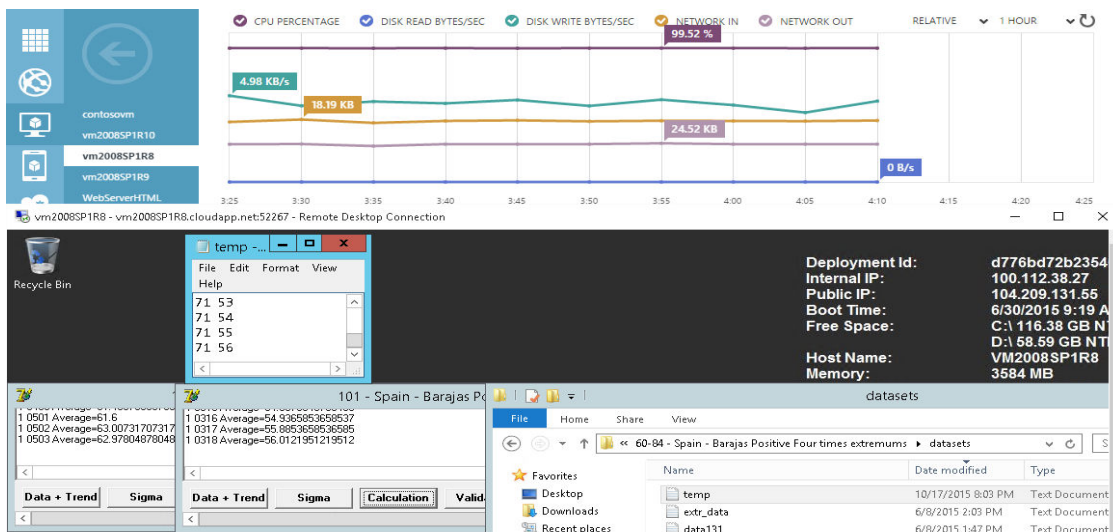


Figure 1. Azure management portal and VM with two Delphi desktop apps



Figure 2. Screenshot of the Google Earth web-site's prototype on the visualization of heat/cold waves

where $s_m \in \{-1, +1\}$ – spin variables indexed by the vertices $V(G)$ of graph G with allowed pairwise interactions given by the edges $E(G)$ of G ; G – graph which represents the topology of quantum processor; $h_m \in [-2, 2]$, $J_{m,n} \in [-1, 1]$ – real-valued weights and dimensionless coefficients, respectively.

Because of h_m and $J_{m,n}$ ranges, the preprocessing standardizes the data using climatological values \bar{x}_{ij} calculated as expectations for the appropriate date from Jan 1, 1973 to Dec 31, 2013:

$$-1 \leq x_{ij}^* = \frac{x_{ij} - \bar{x}_{ij}}{\max |x_{ij} - \bar{x}_{ij}|} \leq 1. \quad (4)$$

For the Ronald Reagan Washington National Airport ($i=114$), $x_{114,4}=39.3^0\text{F}$, $\bar{x}_{114,4}=37.5^0\text{F}$, $\max |x_{ij} - \bar{x}_{ij}|=23.7^0\text{F}$, and hence $x_{114,4}^*=0.076$.

Data (daily mean air temperatures from 119 places around the world as well as sea level at Aburatsu, Japan) are split into learning (from 1975 to 2010: $j = \overline{731,13879}$, 364 extremes for $i=114$) and validation (from 2011 to 2014: $j = \overline{13880,15340}$, 42 extremes for $i=114$) samples. Considering the Ronald Reagan Washington National Airport dataset, positive extremes $x_{114,j_+}^+ \in E$ ($j_+ = \overline{1,364}$, E – set of extremes) are studied on the learning sample.

Model (3) with three qubits is as follows:

$$M(\mathbf{s}|\mathbf{h},\mathbf{J})=2x_{i(j-1)}^*s_1 + 2x_{i(j-2)}^*s_2 + 2x_{i(j-3)}^*s_3 + 0.5(x_{i(j-1)}^* + x_{i(j-2)}^*)s_1s_2 + \\ + 0.5(x_{i(j-1)}^* + x_{i(j-3)}^*)s_1s_3 + 0.5(x_{i(j-2)}^* + x_{i(j-3)}^*)s_2s_3, \quad (5)$$

where $h_1 = 2x_{i(j-1)}^*$; $h_2 = 2x_{i(j-2)}^*$; $h_3 = 2x_{i(j-3)}^*$; $J_{1,2} = 0.5(x_{i(j-1)}^* + x_{i(j-2)}^*)$; $J_{1,3} = 0.5(x_{i(j-1)}^* + x_{i(j-3)}^*)$; $J_{2,3} = 0.5(x_{i(j-2)}^* + x_{i(j-3)}^*)$; $x_{ij}^* \in E$.

Kets $|\mathbf{s}\rangle = |s_1, s_2, s_3\rangle$ represents a 3-day history.

In the forecast algorithm, kets $|\mathbf{s}^*\rangle = |s_1^*, s_2^*, s_3^*\rangle$ together with selected dataset i^* minimize Ising model (3) given $\min\{M(\mathbf{s}^*|\mathbf{h},\mathbf{J})|x_{ij}^* \in E\}$ less than $M(\mathbf{s}^*|\mathbf{h},\mathbf{J})|x_{ij}^* \notin E$. D-Wave One/Two quantum computers may execute the forecast algorithm using one eight-qubit cell only. Several cells can process several data blocks in parallel.

The different number of qubits (from 2 to 5) represent 2-, 3-, 4-, and 5-day historical data, respectively. It was found that qubit individual (e.g. three-qubit individual $\mathbf{s}^* = |s_1^*, s_2^*, s_3^*\rangle$) together with selected dataset i^* minimize Ising model (3) given $M(\mathbf{s}^*|\mathbf{h},\mathbf{J})|x_{ij}^* \in E$ less than $M(\mathbf{s}^*|\mathbf{h},\mathbf{J})|x_{ij}^* \notin E$. The proposed forecast quantum computing algorithm is simulated using the traditional computer architecture and combinatorial optimization of Ising model parameters.

A case study for prediction of the heat waves at Ronald Reagan Washington National Airport shows the operability of the forecast quantum computing algorithm – three-qubit model with ten prediction rules shows 100% forecast accuracy on validation sample. However, the number of identified heat waves is small (only one out of nineteen in this case). Other models with 2, 4, and 5 qubits have 20% (5 prediction rules), 3.8% (41 prediction rules), and 3.8% (84 prediction rules) accuracy, respectively.

The presented three-qubit forecast model is applied for the prediction of the heat waves at other five locations: Aurel Vlaicu, Romania – accuracy is 28.6%; Bratislava, Slovakia – accuracy is

21.7%; Brussels, Belgium – accuracy is 33.3%; Sofia, Bulgaria – accuracy is 50%; Akhisar, Turkey – accuracy is 21.4%. These predictions are not ideal, but not zeros. They can be used independently or together with other predictions generated by different method(s).

4. Connecting Arduino Ethernet Shield and C# console app MQTT subscribers using Mosquitto message broker and publisher

As it was mentioned above, IoT needs the appropriate lightweight protocols to transmit the info because web-protocols (e.g. TCP) generate several times more traffic usually for IoT (e.g. remote connection to the Arduino weather station). MQTT (Message Queuing Telemetry Transport) and CoAP (Constrained Application Protocol) IoT protocols are mainly in use nowadays (<http://postscapes.com/internet-of-things-protocols>). In this activity, Arduino Ethernet Shield and C# console app are connected by MQTT Mosquitto open source software (<http://mosquitto.org>). Similar work presented against <https://iotguys.wordpress.com/2014/11/13/arduino-with-mqtt/>. The activity consists of the following steps:

1. Download and installation of Mosquitto software gainst <http://mosquitto.org/download/>.
 2. Download and installation of the latest Arduino software against <http://arduino.cc/en/main/software>.
 3. Development of the MQTT subscriber based on C programming language in Arduino IDE.
 3. Development of the MQTT subscriber based on C# console app (laptop HP ProBook 650 G1 and Windows 10 are used) in Visual Studio.
- Screen shot of the software is shown in Fig. 3.

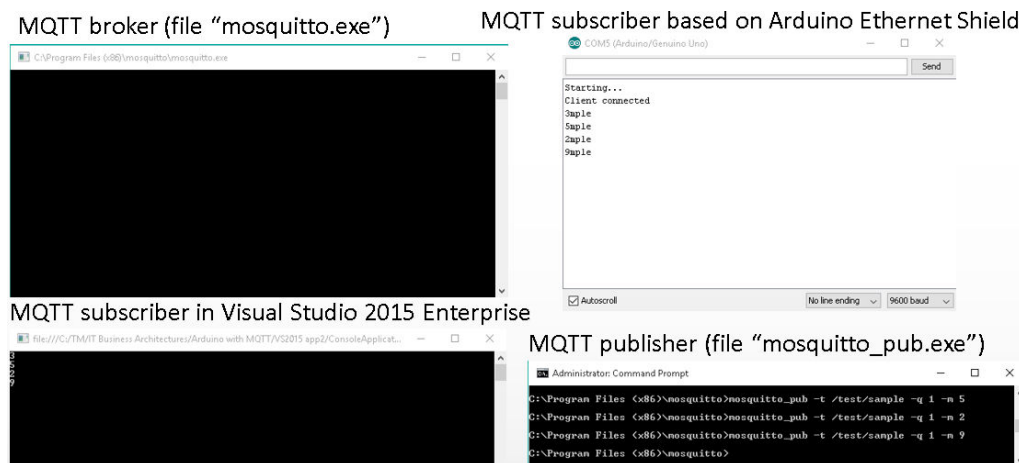


Figure 3. Screenshot of the MQTT broker, publisher, and two subscribers.

5. Conclusions

In this paper, a retrospective study of the non-anticipative analog methodology is presented for the early warning of heat/cold waves. The natural environment subsystem of smart city framework uses this approach to enhance quality of the power grids, the agriculture, the medicine, and other branches.

An Ising model is employed and evaluated for the short-range forecasting of heat waves. The different number of qubits (from 2 to 5) represent 2-, 3-, 4-, and 5-day historical data, respectively. Qubit individual together with selected dataset i^* minimize Ising model (3) given $M(s^*|\mathbf{h},\mathbf{J})|x_{ij}^* \in E$ less than $M(s^*|\mathbf{h},\mathbf{J})|x_{ij}^* \notin E$. The proposed forecast quantum computing algorithm is simulated using the traditional computer architecture and combinatorial optimization of Ising model parameters. The presented three-qubit forecast model is applied for the prediction of the heat waves at six locations: Ronald Reagan Washington National Airport, USA – accuracy is 100%;

Aurel Vlaicu, Romania – accuracy is 28.6%; Bratislava, Slovakia – accuracy is 21.7%; Brussels, Belgium – accuracy is 33.3%; Sofia, Bulgaria – accuracy is 50%; Akhisar, Turkey – accuracy is 21.4%. However, the number of identified heat waves is small (e.g. only one out of nineteen for the Ronald Reagan Washington National Airport).

The classical cloud computation by Windows Azure VMs and data visualization by Google Earth virtual globe are discussed for the non-anticipative long-range forecasting of heat/cold waves. Simulation results show that heat waves can be predicted with accuracy up to 36.4%, cold waves – up to 33.3%. Six high-performance D-series VMs and one A-series standard tier VM with Windows Server 2012 R2 operating system have been used for the reasoning of the forecast models. VMs were hosted in the Windows Azure public cloud. Visualization of the forecasted data is based on Google Earth virtual globe and ASP.NET web-site hosted in Windows Azure public cloud against <http://gearth.azurewebsites.net>. The short- and long-range forecast methods have 100% accuracy with respect to the sign of predicted and actual values.

The experiment with IoT MQTT lightweight protocol using heterogeneous hard- (Arduino Ethernet Shield and HP ProBook 650 G1 laptop) and software (Mosquitto MQTT broker, C# console and Arduino apps) shows the real time operation of the presented approach.

References

- Adelard, L., Boyer, H., Garde, F., & Gatina, J.-C. (2000). Detailed Weather Data Generator for Building Simulations. *Energy and Buildings*, 31, 1, 75-88. doi: 10.1016/S0378-7788(99)00009-2
- Amin, M.H.S., Neil G. Dickson, Peter Smith (2013). *Adiabatic quantum optimization with qubits*. Quantum Information Processing, Apr 2013, Vol. 12, Iss. 4, Springer, 2013, pp. 1819-1829.
- Astahova, E.D., & Alferov, Y.V. (2008). High Performance Version of the Atmosphere Spectral Model for Deterministic and Ensemble Weather Forecast' Design using Multiprocessor Systems. *J. of Russian Hydrometcentre*, 342, 118-133.
- Bardin, M.Y. (2011). Scenario forecasts of air temperature variations for the regions of the Russian Federation up to 2030 using the empirical stochastic climate models. *Russian Meteorology and Hydrology J.*, 36, 217-228.
- Belov, P.I., Borisenkov, E.P., & Panin, B.D. (1989). *Numerical Methods of Weather Prediction*. Leningrad: Gidrometeoizdat Press.
- Charalampos Doukas (2012). *Building Internet of Things With the Arduino*. Seattle, Washington, United States: Amazon.com, CreateSpace Independent Publishing Platform.
- Collier, M., Shahan, R. (2015). *Microsoft Azure Essentials*. Washington: Microsoft Press.
- Dahl, E.D. (2015). *Quantum Computing 101. Machine Design*. Retrieved from <http://machinedesign.com/technologies/quantum-computing-101>
- Dirk Slama, Frank Puhlmann, Jim Morrish, Rishi M. Bhatnagar (2015). *Enterprise IoT: Strategies and Best Practices for Connected Products and Services*. California, United States: O'Reilly Media.
- Douglas, Arthur V., & Phillip J. Englehart. (2007). A Climatological Perspective of Transient Synoptic Features during NAME 2004. *J. Climate*, 20, 1947-1954. doi: 10.1175/jcli4095.1
- Fathalla A. Rihan, & Chris G. Collier. (2010). A Basis for Improving Numerical Forecasting in the Gulf Area by Assimilating Doppler Radar Radial Winds. *Int. J. of Geosciences*, 1, 70-78. doi:10.4236/ijg.2010.12010
- Glantz, M.H., Katz, R.W., & Nicholls, N. (Eds.) (1991). *Teleconnections Linking Worldwide Climate Anomalies*. Cambridge University Press.
- Gyanesh Shrivastava, Sanjeev Karmakar, Manoj Kumar Kowar, & Pulak Guhathakurta (2012). Application of Artificial Neural Networks in Weather Forecasting: A Comprehensive Literature Review. *Int. J. of Computer Applications*, 51, 17-29. doi: 10.5120/8142-1867

- HafedhChourabi, Taewoo Nam, Shawn Walker, J. Ramon Gil-Garcia, SehlMellouli, KarineNahon, Theresa Pardo, & Hans Jochen Scholl (2012). Understanding Smart Cities: An Integrative Framework. *45th Hawaii International Conference on System Sciences*, 2289-2297. doi: 10.1109/HICSS.2012.615
- Higgins, R.W., Kim, H-K., & Unger, D. (2004). Long-Lead Seasonal Temperature and Precipitation Prediction Using Tropical Pacific SST Consolidation Forecasts. *J. Climate*, 17, 3398-3414. doi: 10.1175/1520-0442(2004)017<3398:LSTAPP>2.0.CO;2
- Kattsov, V.M. (2010). Climate prediction: Progress, Problems, and Prospects. *Russian Meteorology and Hydrology J.*, 35, 10-12. doi: 10.3103/s1068373910010024
- Kelly L. Murdock (2009). *Google SketchUp and SketchUp Pro 7 Bible*. Indianapolis: Wiley Publishing.
- Luis Hernández, Carlos Baladrón, Javier M. Aguiar, Lorena Calavia , BelénCarro, Antonio Sánchez-Esguevillas, Diane J. Cook, David Chinarro, & Jorge Gómez (2012). A Study of the Relationship between Weather Variables andElectric Power Demand inside a Smart Grid/Smart WorldFramework. *Sensors J.*,12, 11571-11591. doi:10.3390/s120911571
- Madala, H.R., &Ivakhnenko, A.G. (1994). *Inductive Learning Algorithms for Complex Systems Modeling*. Boca Raton: CRC Press.
- McGeoch, C., Wang, C. (2013). Experimental Evaluation of an Adiabatic Quantum System for Combinatorial Optimization. *CF 2013*, 023:1-023:11.
- Nada PavlovicBerdon. (2013). The Impact of Teleconnection on Pressure, Temperature and Precipitation in Serbia. *Int. J. of Remote Sensing Applications*, Vol. 3, Iss. 4, 185-192. doi: 10.14355/ijrsa.2013.0304.03
- Onwubolu, G.C., Buryan, P., Garimella, S., Ramachandran, V., Buadromo, V., & Abraham, A. (2007). Self-organizing Data Mining for Weather Forecasting. *IADIS European Conf. Data Mining*, 81-88.
- Qiang Song (2011). Average Power Function of Noise and Its Applications in Seasonal Time Series Modeling and Forecasting. *American J. of Operations Research*, 1, 293-304. doi:10.4236/ajor.2011.14034
- Sadokov, V.P., Kozelcova, V.F., &Kuznecova, N.N. (2011). Probabilistic Forecast of Warm and Cold Weather in Belorussia. *J. of Russian Hydrometcentre*, 345, 144-154.
- Smart Weather Solutions* (2013). Retrieved from Schneider Electric SE Corporation: http://www.schneider-electric.com.co/documents/local/xperience-efficiency/Smart_Weather_Solutions.pdf
- Smelyanskiy, V.N., Rieffel, E.G., Knysh, S.I., Williams, C.P., Johnson, M.W., Thom, M.C., Macready, W.G., &Pudenz, K.L. (2012). *A Near-Term Quantum Computing Approach for Hard Computational Problems in Space Exploration*. arXiv:1204.2821.
- Tyndall, Daniel P., John D. Horel, & Manuel S. F. V. de Pondecá. (2010). Sensitivity of Surface Air Temperature Analyses to Background and Observation Errors. *Wea. Forecasting J.*, 25, 852-865. doi: 10.1175/2009waf2222304.1
- Van Den Dool, H. M., & Nap, J. L. (1985). Short and Long Range Air Temperature Forecast near an Ocean. *Mon. Wea. Rev. J.*, 113, 878-886. doi: 10.1175/1520-0493(1985)113<0878:SALRAT>2.0.CO;2
- Valerie Lampkin, Weng Tat Leong, Leonardo Olivera, SwetaRawat, NageshSubrahmanyam, Rong Xiang (2012). *Building Smarter Planet Solutions with MQTT and IBM WebSphere MQ Telemetry*. Retrieved fromInternational Business Machines Corporation: <http://www.redbooks.ibm.com/redbooks/pdfs/sg248054.pdf>
- Vilfand, R.M., Tishenko, V.A., & Khan, V.M. (2003). Surface Air Temperature's Forecast with Month Lead Time using Ensemble Approach. *Gidrometeoizdat Press, Fundamental and Applied Hydrometeorological Research*, 3-13.
- Vorobiov, V.I. (1991). *Synoptic meteorology*. Leningrad: Gidrometeoizdat Press.

- Zubov, D. (2013). Average Daily Air Temperature's Long-Range Forecast Using Inductive Modeling and Satellite Datasets. *Proc. of joint 2013 EUMETSAT Meteorological Satellite and 19th American Meteorological Society Satellite Meteorology, Oceanography, and Climatology Conferences, Vienna, Austria, Sept 16-20, 2013.* doi: 10.13140/RG.2.1.3635.9524. Retrieved from http://www.eumetsat.int/website/home/News/ConferencesandEvents/DAT_2027670.html
- Zubov, D.A., & Vlasov, Y.N. (2004). Long-Term Forecasting of the Air Average Temperature and Atmospheric Precipitations Using the Linear Auto Regression Model and Maximal Error's Minimization Objective Function. *Scientific J. of V.Dahl East Ukrainian National University*, 40-49.
- Zubov, D. (2015). Cloud Computation of Nonanticipative Analogs for Heat/Cold Waves Teleconnections. *European Cooperation J.*, N 1, 84-94. Retrieved from <http://we.clmconsulting.pl/index.php/we/article/view/22/36>